ACS SENSORS

pubs.acs.org/acssensors
Article

Extremely Sensitive Genetically Encoded Temperature Indicator Enabling Measurement at the Organelle Level

Shun-ichi Fukushima, Tetsuichi Wazawa, Kazunori Sugiura, and Takeharu Nagai*

Cite This: ACS Sens. 2024, 9, 3889−3897
Read Online

ABSTRACT: Intracellular temperature is a fundamental parameter in biochemical reactions. Genetically encoded fluorescent temperature indicators (GETIs) have been developed to visualize intracellular thermogenesis; however, the temperature sensitivity or localization capability in specific organelles should have been further improved to clearly capture when and where intracellular temperature changes at the subcellular level occur. Here, we developed a new GETI, gMELT, composed of donor and acceptor subunits, in which cyan and yellow fluorescent proteins, respectively, as a Förster resonance energy transfer (FRET) pair were fused with temperature-sensitive domains. The donor and acceptor subunits associated and dissociated in response to temperature changes, altering the FRET efficiency. Consequently, gMELT functioned as a fluorescence ratiometric indicator. Untagged gMELT was expressed in the cytoplasm, whereas versions fused with specific localization signals were targeted to the endoplasmic reticulum (ER) or mitochondria. All gMELT variations enabled more sensitive temperature measurements in cellular compartments than those in previous GETIs. The gMELTs, tagged with ER or mitochondrial targeting sequences, were used to detect thermogenesis in organelles stimulated chemically, a method previously known to induce thermogenesis. The observed temperature changes were comparable to previous reports, assuming that the fluorescence readout changes were exclusively due to temperature variations. Furthermore, we demonstrated how macromolecular crowding influences gMELT fluorescence given that this factor can subtly affect the fluorescence readout. Investigating thermogenesis with gMELT, accounting for factors such as macromolecular crowding, will enhance our understanding of intracellular thermogenesis phenomena.

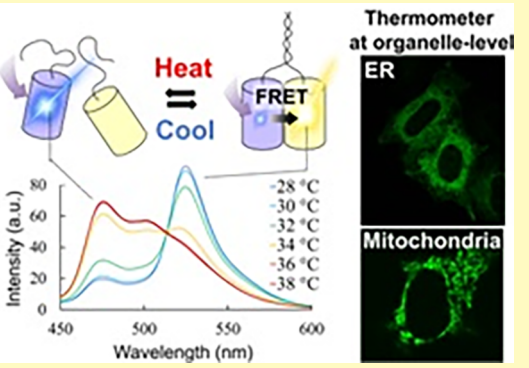

KEYWORDS: *fluorescent protein, fluorescence nanothermometry (FNT), genetically encoded fluorescent temperature indicator (GETI), protein engineering, biosensor*

Body temperature is a crucial parameter that determines the biological activity of every organism. Especially in homeotherms, not only the environmental temperature but also endogenous biochemical reactions involving heat are important for life support. For example, human body conditions are substantially affected if the body temperature deviates by as little as ∼1 °C due to, e.g., fever. This is clear evidence that small internal thermogenesis significantly affects biochemical reactions and health conditions. Capturing endogenous temperature increases and decreases at the cellular and organelle levels should lead to a better understanding of the mechanisms of temperature homeostasis and to a reconsideration of changes in intracellular conditions caused by local temperature fluctuations, which have not been well investigated in conventional biological studies.

Fluorescence nanothermometry (FNT) allows for the monitoring of temperature dynamics in living cells with high spatial and temporal resolutions. In the FNT of cells, probes that change fluorescence in a temperature-dependent manner are introduced into cells to measure the intracellular temperature through the fluorescence signals. Various temperature-responsive compounds including organic dyes, nanoparticles, nanodiamonds, cationic polymers, oligonucleotides, and fluorescent proteins (FPs) have been used to develop fluorescent temperature indicators for FNT.[1−4] An early leading study reported local thermogenesis induced by a proton uncoupler in the region that overlapped with the locations of mitochondria, as investigated by an organic polymer-based thermometer loaded in the whole cell region.[5] Following a study suggesting the possibility of subcellular thermogenesis,[5] a number of temperature indicators that can localize in specific organelles have been developed, and temperature increases have been observed in local intracellular

Received: December 11, 2023
Revised: July 18, 2024
Accepted: July 19, 2024
Published: July 23, 2024

https://doi.org/10.1021/acssensors.3c02658
ACS Sens. 2024, 9, 3889−3897

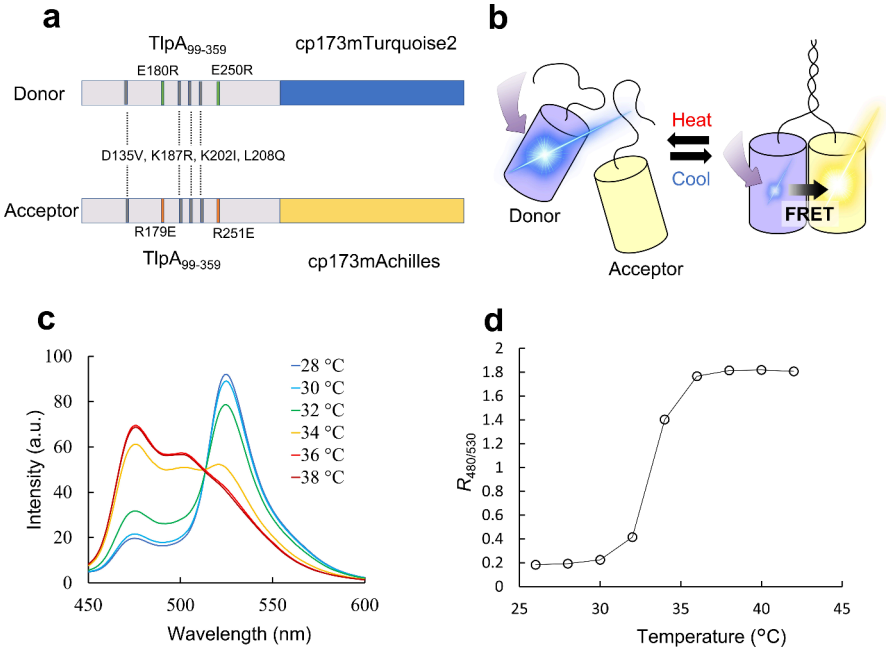

Figure 1. Design and temperature responses of gMELT. (a) Schematic diagrams of gene design of gMELT. (b) The operating principle of gMELT. (c) Fluorescence emission spectra of gMELT at various temperatures. The purified donor subunit (1 μM) and acceptor subunit (2 μM) were dissolved in PBS (pH 7.4). The excitation wavelength was 405 nm. (d) A plot of the fluorescence ratio of CFP (480 nm) and YFP (530 nm) against temperature. The protein concentration and buffer condition were the same with panel c. Data are represented as the mean ± SD (n = 3).

compartments, such as the mitochondria[6−11] and endoplasmic reticulum (ER).[6,12]

Irrespective of the tantalizing suggestions for temperatures, it is still very challenging to detect such temperature increases at the single-cell level using previously known fluorescent temperature indicators mainly because of their low temperature sensitivity.[1] In fact, the temperature sensitivity ($St = (1/S)\cdot(\Delta S/\Delta T)$) of the temperature indicators has been < several %/°C, where S is a fluorescence signal and ΔS is a change of S caused by a temperature change ΔT. To resolve this problem, we previously reported ELP-TEMP,[13] a genetically encoded temperature indicator (GETI) that showed high sensitivity (St = 19.5 ± 5.0 and 45.1 ± 8.1%/°C in the cytoplasm and nucleus, respectively) to temperature changes. This GETI was composed of cyan fluorescent protein (CFP), yellow fluorescent protein (YFP), and a thermosensitive domain derived from an elastin-like polypeptide (ELP) that reversibly formed intermolecular coacervates in a temperature-dependent manner. In ELP-TEMP, at high temperatures, the ELP domain formed intermolecular coacervates such that the distance between the CFP and YFP decreases, leading to a high Förster resonance energy transfer (FRET) efficiency. At a low temperature, the coacervates disassembled, resulting in a low FRET efficiency. Thus, a large change in the FRET efficiency allowed for highly sensitive temperature detection. An advantage of genetically encoded indicators is their capability for versatile and specific targeting to a cellular compartment by genetically fusing the indicator and a known specific amino acid signal sequence.[6,9,10] In fact, GETIs, such as tsGFP, gTEMP, and emGFP, have allowed for specific localization to cellular compartments. However, localizing ELP-TEMP specifically to targeted cellular compartments seems to be challenging due to its large molecular size (104.6 kDa) and its ability to form organelle-sized coacervate through multimolecular interaction.[14] Thus, the compatibility of high-sensitivity temperature measurements and versatile localization to a specific target is a challenge in the discovery of thermogenesis phenomena.

In this study, we developed a new FRET-based GETI that was the most temperature-sensitive ever and can specifically localize in the cytoplasm, ER, and mitochondria. We designed the current GETI using fluorescent proteins and temperature-sensitive coiled-coil domains. We confirmed the temperature sensitivity of the fluorescence ratio measured from the GETI in vitro and evaluated its cross talk with factors other than temperature. We also confirmed its temperature sensitivity in the cytoplasm, ER, and mitochondria. Furthermore, we tried to detect intracellular thermogenesis induced by drug stimulation.

MATERIALS AND METHODS

Gene Construction. For the gene construction of circularly permutated (cp) 173 variants of mTurquoise2[15] and Achilles,[16] the sequences encoding the N- and C-terminal domains containing the sequence encoding the linker (GGSGG) in the 5′ and 3′ ends, respectively, were individually amplified by PCR, and the fragments were introduced into pRSETb in the same order as cp173Venus[17] using the hot-fusion method.[18] DNA fragments of the cp173 variants and tlpA were amplified by PCR and fused with pRSETb using the hot-fusion method. All point mutations described in Figure 1a were introduced using the hot-fusion method for constructing the donor and acceptor subunits of gMELT. To construct gMELT-Cyto, PCR products for the donor subunit, the acceptor subunit, and coding sequences for GSG-P2A (GSGATNFSLLKQAGDVEENPGP) were introduced into pcDNA3.1(−) in the order donor−GSG−P2A−acceptor using the hot-fusion method.[18] To construct gMELT-ER, the targeting sequences derived from calreticulin (MLLSVPLLLGLLGLAVA) and the ER retrieval sequence (KDEL) were fused at the N- and C-termini, respectively, in both the donor and acceptor domains. The coding sequence of furin (RKRR) was introduced just upstream of P2A for effective localization.[19] In gMELT-Mito, the signal peptide from subunit VIII of cytochrome c oxidase (COX) (MSVLTPLLLRGLTGSARRLPVPRAKIHSLP-PEGKLG) was tandemly fused to the N-terminal sides of both the

https://doi.org/10.1021/acssensors.3c02658
ACS Sens. 2024, 9, 3889−3897

donor and acceptor domains. The DNA sequences of gMELT variants are shown in Note S2. All of the gene constructions were transformed into XL-10 Gold *E. coli* cells (200314, Agilent Technologies) and cultured in the lysogeny broth (LB) medium with 100 μg/mL carbenicillin (Sigma-Aldrich) overnight at 37 °C, and the plasmids were purified.

Protein Purification. *E. coli* strain JM109 (DE3) was transformed with the pRSET$_B$ plasmid encoding the donor or acceptor subunit of gMELT. The transformed cells were cultured in 500 mL of LB medium containing 100 μg/mL carbenicillin overnight at 37 °C. The collected cell leakage expressing the His-tagged donor or acceptor subunit of gMELT was suspended in ice-cold phosphate-buffered saline solution (PBS) (pH 7.4) containing a protease inhibitor cocktail (Roche Diagnostics) and ultrasonicated on ice. After centrifugation, the supernatant was subjected to Ni-NTA affinity chromatography using Ni-NTAagarose resin (Qiagen). The resin was washed with TN buffer (10 mM Tris-HCl and 150 mM NaCl, pH 8.0) containing 10 mM imidazole and eluted using the same buffer containing 100 mM imidazole. The eluates were applied to a PD-10 desalting column (Cytiva) equilibrated with PBS, and the fraction containing the protein was collected.

Fluorescence Spectroscopy Measurement. Fluorescence emission spectra were measured using an FP-750 spectrofluorometer (JASCO) equipped with a temperature controller unit (ETC-272T, JASCO) and a quartz cuvette. The excitation wavelength was 405 nm. When necessary, the solution containing purified gMELT was supplemented with Ficoll PM70 (Sigma-Aldrich), $CaCl_2$, $MgCl_2$, or 1 mM EDTA. For pH dependence measurement, mixtures of 30 mM trisodium citrate and 30 mM borax adjusted to pH 6.0−8.0 by adding HCl were used. To examine gMELT performance in heating−cooling cycles, we measured its fluorescence between 26 and 38 °C. We adjusted the solution's temperature at a rate of 5 °C/min. The temperature was stabilized for 5 min at each point before measurement.

Cell Culture and Transfection. HeLa cells were cultured in Dulbecco's modified Eagle's medium (Sigma-Aldrich) supplemented with 10% fetal bovine serum (Biowest) at 37 °C in a 5% CO_2 incubator. The cells were seeded on homemade 35 mm glass-bottom dishes coated with collagen (Cellmatrix Type I-C, Nitta Gelatin) and transfected using polyethylene imine (PEI Max 40K; Polysciences) with pcDNA3.1(−) coding for each required gene according to the manufacturer's instructions.

Temperature Imaging in HeLa Cells. Cells transfected with the plasmid encoding gMELT were cultured for approximately 48 h, and the medium was replaced with DMEM/F12 (11039-021, Thermo Fisher Scientific) without phenol red before microscopic observation. For observation, an inverted microscope (Ti-2 Eclipse, Nikon) equipped with a confocal unit (Dragonfly 200, Andor Technology), a microscope objective (CFI Plan Apochromat λ 60× Oil; numerical aperture, 1.40; Nikon), and a stage-top incubator with 5% CO_2 supply (STXG-WSKMX, Tokai Hit) were used. Laser beam at 445 nm was used to excite gMELT. Fluorescence emission through bandpass filters (ET480/40 and ET540/30 nm for CFP and YFP, respectively; Chroma) was captured by an EMCCD camera (iXon Ultra DU-888U3-CS0-#BV, Oxford Instruments) with 500 ms exposure time. The background was subtracted from each captured raw image for analysis because the appropriate background subtraction was essential for ratiometric imaging. The temperature of the medium was monitored using a temperature controller in a stage-top incubator (STX App, Tokai Hit) and was controlled using an in-house perfusion system. Optics and material preparation for local quick heating using carbon nanotubes (CNTs) followed a previous report.[13]

Observation of gMELT Localized in ER and Mitochondria. HeLa cells transfected with plasmids encoding gMELT-Mito or gMELT-ER were stained with 100 nM MitoTracker Red CMXRos (M7512, Invitrogen) or ER-Tracker Red (E34250, Invitrogen) and suspended in DMEM/F12 for 30 min in an incubator. The medium was then exchanged with dye-free DMEM/F12. To detect fluorescence from MitoTracker and ERTracker, a 561 nm laser and a band-pass filter (ET600/50 nm, Chroma) were used for excitation and emission, respectively. To observe the localization of YFP by direct excitation, a 514 nm laser and band-pass filter (ET540/30 nm, Chroma) were used for excitation and emission, respectively. For differential interference contrast (DIC) imaging, a polarizer, an objective Nomarski prism, and an analyzer installed in the Ti-2 Eclipse microscope were set up according to the manufacturer's instructions.

Observation of Intracellular Thermogenesis Induced by Chemical Stimulation. HeLa cells were transfected with plasmids encoding gMELT-Mito or gMELT-ER. The cells expressing gMELT-Mito or gMELT-ER were stimulated with 10 μM FCCP or 5 μM ionomycin, respectively, by using a perfusion system.

RESULTS AND DISCUSSION

Design of a GETI, gMELT. To construct a highly sensitive GETI, we used the TlpA domains, which were derived from a temperature-sensitive transcriptional repressor from *Salmonella typhimurium*[20] and were used in a pioneering GETI, tsGFP.[6] For tsGFP, ancestral GFP (avGFP) was genetically fused to the coiled-coil subdomain of TlpA. TlpA undergoes homodimeric binding and dissociation at low and high temperatures, respectively, and this concurrent structural change affects the protonation state of the GFP chromophore, leading to a change in the absorption spectrum. A possible reason for the low temperature sensitivity for tsGFP (St = 3.9%/°C estimated from the figure in the report[6]) in cytoplasm of HeLa cells despite the large conformational change of the TlpA domain would be that the temperature-dependent structural change of the TlpA domain does not effectively influence the chromophore protonation state in tsGFP to induce a large fluorescence signal change.

To solve this problem, we aimed at enhancing the temperature sensitivity of GETI using FRET. We designed a GETI composed of donor and acceptor subunits such that CFP and YFP, respectively, were fused with temperature-sensitive domains originating from TlpA containing different mutations (Figure 1a,b). Specifically, we used circularly permutated (cp) 173 variants of mTurquoise2[15] and Achilles[16] for CFP and YFP, respectively (Figure 1a).[21] We postulated that the distance between CFP and YFP decreased because of the weak dimer formation in the presence of both donor and acceptor subunits at low temperatures, which was expected to result in low and high fluorescence from CFP and YFP, respectively, due to FRET (Figure 1b). As the donor and acceptor subunits dissociate with increasing temperature, the YFP emission was expected to decrease and the CFP emission to increase. Because of the homodimer formation ability of native TlpA, if native TlpA was used for the donor and acceptor subunits, dimerization between the two donor subunits or two acceptor subunits could also occur, which should result in a lower FRET efficiency between CFP and YFP. To prevent the homodimer formation, Piraner et al. developed a pair of TlpA-derived proteins with different amino acid mutations to form heterodimers,[22] and thereby, we introduced these mutations into the donor and acceptor subunits (Figure 1a). Piraner et al. also reported some mutations such that the transition temperature of TlpA fitted the biological temperature range in mammals;[23] thus, we also introduced these mutations into our GETI. We denote the present design of GETI as gMELT (Genetically encoded system to Monitor the Events of Local Temperature).

Thermoresponsivity of gMELT In Vitro. To evaluate the temperature sensitivity of gMELT, the purified donor and acceptor subunits were mixed at concentrations of 1 and 2 μM,

https://doi.org/10.1021/acssensors.3c02658
ACS Sens. 2024, 9, 3889−3897

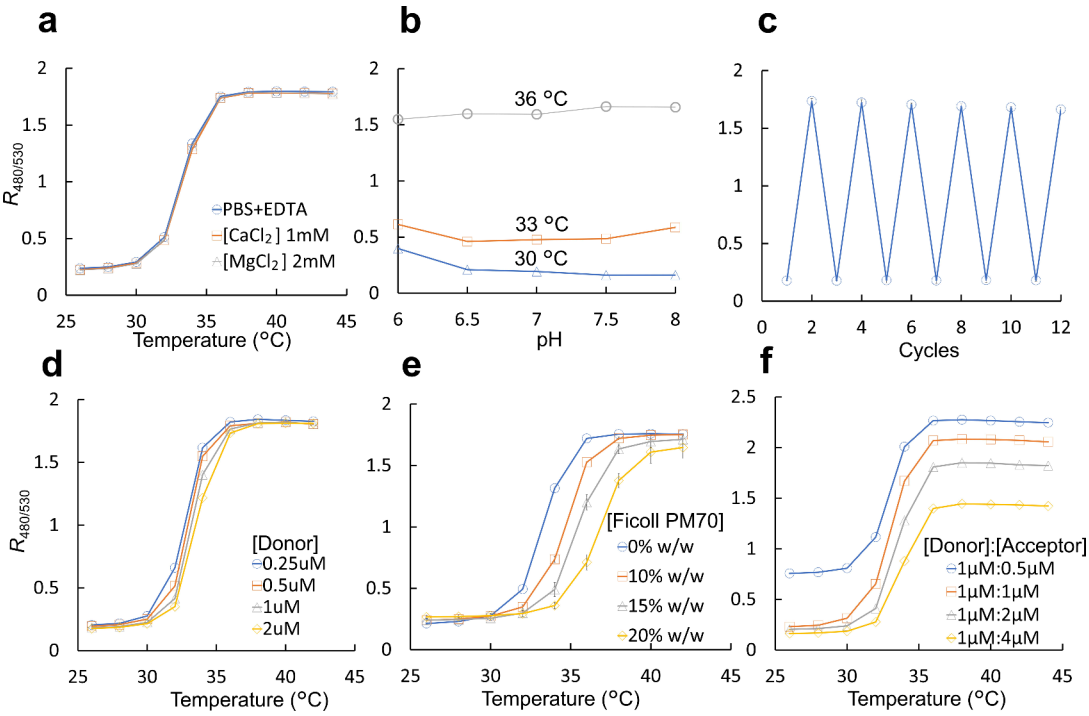

Figure 2. Fluorescence response of gMELT to temperature in various conditions. (a) The effect of $CaCl_2$ or $MgCl_2$ on the temperature response of gMELT. (b) pH dependence of gMELT fluorescence ratio at several temperatures. The gMELT solution contained 30 mM trisodium citrate and 30 mM borax whose pH was adjusted by adding HCl. (c) The reversibility of gMELT fluorescence ratio in repeated cycles of temperature increase and decrease. (d) The effect of self-concentration of gMELT on its temperature dependence of the fluorescence ratio. (e) The effect of Ficoll PM70 on the temperature dependence of the fluorescence ratio. (f) The temperature dependence of gMELT fluorescence at various molar ratios of the donor and acceptor subunits. Purified donor subunit (1 μM) and acceptor subunit (concentrations indicated in the panel) were dissolved in PBS (pH 7.4) with the required supplements unless otherwise mentioned. The excitation wavelength was 405 nm. Data are represented as mean ± SD (n = 3).

respectively, and changes in the emission spectra excited at 405 nm in a phosphate-buffered saline solution (PBS) were measured in response to increasing temperature. At a low temperature, e.g., 28 °C, the mixture of the purified donor and acceptor subunits showed fluorescence emission bands at 480 and 530 nm (Figure 1c), which correspond to the fluorescence of CFP and YFP, respectively. This indicated that dimerization of the TlpA domains in the donor and acceptor subunits occurred, and thus, FRET from CFP to YFP took place (Figure 1b). In contrast, at a high temperature, e.g., 38 °C, the mixture of the donor and acceptor subunits mostly exhibited the fluorescence emission of CFP (Figure 1c), which indicates the vanishing of the FRET due to the unbinding of the TlpA domains (Figure 1b). The fluorescence ratio of the fluorescence intensity of the 480 nm band to that of the 530 nm band, $R_{480/530}$, changed by 8.6-fold for a temperature increase from 30 to 36 °C (Figure 1d), indicating that gMELT is applicable for temperature measurement with high sensitivity.

Furthermore, we examined the effects of variations in solution conditions on the fluorescence response and reversibility of gMELT. The presence of Ca^{2+} or Mg^{2+} at a physiological concentration did not affect the temperature response of gMELT (Figure 2a). The pH titration curves in Figure 2b show that $R_{480/530}$ at 30, 33, and 36 °C did not significantly change between pH 6.5 and 8.0. The change of $R_{480/530}$ was highly reversible in repeated cycles of temperature increase and decrease (Figure 2c). We previously reported the temperature dependence of ELP-TEMP on the self-concentration and concentration of Ficoll PM70,[13] which is widely used as a standard reagent that mimics intracellular macromolecular crowding.[24] In the case of gMELT, self-concentration dependency of the transition temperature was observed to a small degree (Figure 2d), but the dependency was much smaller than that of ELP-TEMP. In the case of ELP-TEMP, the temperature-sensitive range decreased by about 15 °C in response to the addition of 14% Ficoll PM70, and this was consistent with its temperature dependence when expressed in the cytoplasm,[13] whereas in the case of gMELT, the temperature-sensitive range increased only by 2−3 °C with the addition of 15% Ficoll PM70 (Figure 2e) so that the temperature-sensitive range was closer to mammalian growth temperature with the Ficoll PM 70. Thus, the influence of the self-concentration and macromolecular crowding on the temperature response of gMELT was much smaller than that of ELP-TEMP in vitro,[13] probably due of the difference in the thermosensitive domains: the elastin-like polypeptide employed by ELP-TEMP aggregates in multiple molecules in a temperature-dependent manner, whereas TlpA employed by gMELT dimerizes between paired two molecules.[22] Although we used a HeLa cell line with homogeneous and stable ELP-TEMP expression to reduce the influence of self-concentration variations in ELP-TEMP in our previous report,[13] gMELT solved this problem as shown below (see Thermoresponsivity of gMELT in HeLa cells). On the other hand, for accurate cellular temperature measurement, it is essential to account for the persistent sensitivity to macromolecular crowding.

Finally, we examined the temperature dependence of the stoichiometric ratio of the donor and acceptor subunits (Figure 2f). At a constant donor subunit concentration of 1 μM,

https://doi.org/10.1021/acssensors.3c02658
ACS Sens. 2024, 9, 3889−3897

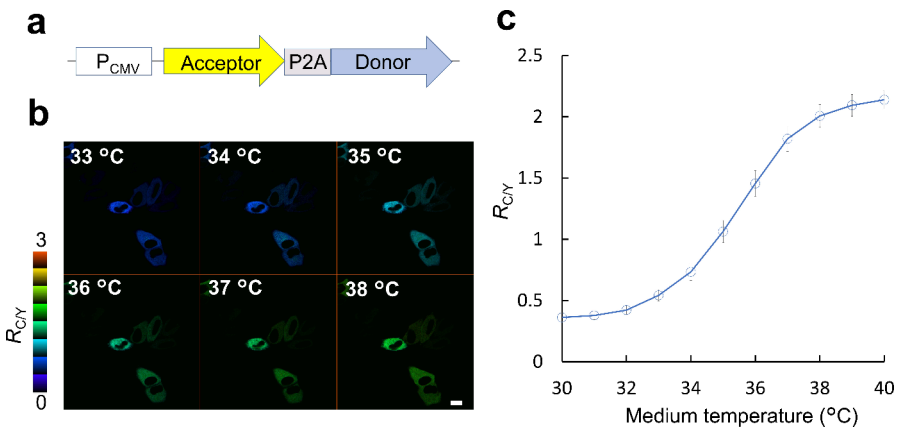

Figure 3. Expression system and temperature sensitivity of gMELT in HeLa cells. (a) The schematic diagram of gene design for bicistronic expression of donor and acceptor subunits via P2A in HeLa cells. (b) Pseudocolor images of HeLa cells expressing gMELT in the cytoplasm with respect to the fluorescence ratio $R_{C/Y}$ (CFP/YFP) at various medium temperatures. $R_{C/Y}$ was calculated from the emission from CFP (480 ± 20 nm) and YFP (540 ± 15 nm) excited at 445 nm under a confocal microscope. (c) A plot of the fluorescence ratio against medium temperature. Scale bar, 10 μm. Data are presented as the mean ± SD (n = 28).

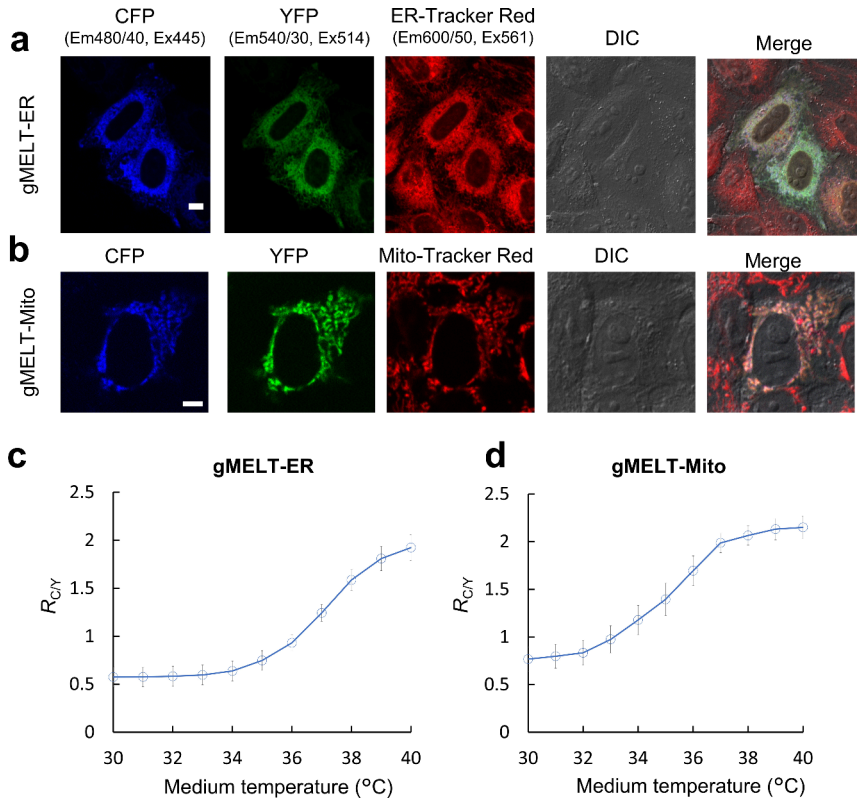

Figure 4. Localization in ER and mitochondria and the temperature sensitivity of gMELT expressed in HeLa cells. (a, b) Confocal images of HeLa cells expressing (a) gMELT-ER and (b) gMELT-Mito. Scale bars are 10 μm. Both donor and acceptor subunits were colocalized with ER-Tracker Red in panel a and Mito-Tracker Red in panel b. (c, d) Temperature-dependent fluorescence ratios $R_{C/Y}$ of gMELT-ER (c) and gMELT-Mito (d) in HeLa cells. Data are represented as mean ± SD (n = 35 and 19 cells for panels c and d, respectively).

$R_{480/530}$ at each temperature decreased as the acceptor concentration increased, suggesting that the increase of the apparent FRET efficiency was due to the increased fraction of the donor subunit bound to the acceptor subunit. However, the temperature-sensitive range remained virtually unchanged. These results suggest that at a constant stoichiometric ratio of donor and acceptor subunits, gMELT responds to temperature change in a robust manner.

Thermoresponsivity of gMELT in HeLa Cells. We tested the temperature response of gMELT in the live HeLa cells. For the stoichiometric expression of the donor and acceptor subunits, we employed a P2A-based bicistronic expression system[25] (Figure 3a). The P2A system commonly facilitates the expression of proteins encoded both upstream and downstream of the P2A sequence in a fixed ratio. Typically, the expression level of the upstream tends to be slightly higher than that of downstream. When we observed transiently expressed gMELT in HeLa cells with excitation at 445 nm using a confocal microscope, the fluorescence from CFP and YFP was captured in the cytoplasm, indicating that CFP and

https://doi.org/10.1021/acssensors.3c02658
ACS Sens. 2024, 9, 3889−3897

YFP were both expressed (Figure 3a). We denote this version of gMELT as gMELT-Cyto. When the medium temperature was increased without any other stimulus, the fluorescence from CFP increased, and that from YFP decreased. As shown in Figure 3b, the ratio of the fluorescence intensity of the CFP channel to that of the YFP channel, $R_{C/Y}$, clearly changed in response to temperature change, indicating that gMELT-Cyto can report cytoplasmic temperature changes. *St* of gMELT-Cyto was >10%/°C between 31 and 37 °C, and the maximum *St* was 39.3 ± 6.0%/°C at 34 °C (Figure 3c).

To assess the response speed of gMELT to temperature changes, we exposed cells expressing gMELT-Cyto to an abrupt shift in temperature induced by CNT heating (Figure S1 and Movie S1). During the cycles of activating and deactivating the CNT heating, we noted an increase in $R_{C/Y}$ during heating and a decrease during pause (Figure S1a). We analyzed the time trajectories of $R_{C/Y}$ ($\Delta R_{C/Y}$) in regions minimally affected by light leakage from the nearby CNT cluster heating (Figure S1b). By least-squares fitting analysis on the $R_{C/Y}$ time trajectory from ROI2 in Figure S1a using single exponential function, the time constants were 0.093 ± 0.005 and 0.252 ± 0.035 s (mean ± SE, n = 3) for the rising and falling phases, respectively. These time constants may primarily reflect the dissociation and association rates of the donor and acceptor subunits. The response speed to temperature changes varies among temperature indicators: Lu et al. reported a GETI of B-gTEMP that responded to an abrupt temperature change in less than a millisecond;[26] Nwokolo et al. described a fluorescent ratiometric "memory-based calorimeter" that responded more slowly to temperature decrease than increases, thus functioning as an integral sensor for heat production events.[27] gMELT functions as a thermometer rather than a calorimeter given its reversible response to both increases and decreases in temperature on a subsecond time scale.

Moreover, we tried to observe the localization of gMELT. We fused both the donor and acceptor subunits to specific organelle-targeting sequences to yield gMELT-ER and gMELT-Mito, which were aimed at localizing in the ER and mitochondria, respectively. To confirm the localization, cells expressing gMELT-ER or gMELT-Mito were stained with ER- or MitoTracker Red, whose fluorescence emission bands were almost separate from the band wavelengths of the CFP and YFP channels. As shown in Figure 4a,b, the fluorescence from CFP and YFP well colocalized with that from ER- or Mito-Tracker Red. Furthermore, we observed that $R_{C/Y}$ increased with an increasing medium temperature and without any other stimulus (Figure 4c,d), confirming that gMELT also functioned as a temperature indicator in the ER and mitochondria. The maxima of *St* for gMELT-ER and gMELT-Mito were 33.8 ± 4.6%/°C at 36 °C and 22.0 ± 4.5%/°C at 35 °C, respectively. It should be noted that the sensitivity of gMELT greatly surpassed previously reported GETIs (e.g., ELP-TEMP, *St* = 19.5%/°C in cytoplasm;[13] tsGFP-ER, *St* = 2.8%/°C in ER;[6,10] emGFP-mito, *St* = 2.2%/°C in mitochondria[10]).

The response temperatures of gMELT and its variants in cytoplasm, ER, and mitochondria in the steady state were slightly different (Figures 3c and 4c,d), and the transition temperatures showed the same tendency (ER > cytoplasm ≥ mitochondria) with tsGFPs,[6] which contained a thermosensitive domain originating from TlpA like gMELT. The difference in transition temperatures may have reflected slight variations in the compartment's temperatures. However, our studies with GETIs such as ELP-TEMP and B-gTEMP indicated that these temperature differences, particularly in the cytoplasm and nucleus, were too small to be detected.[13,26] Furthermore, our experiments with gMELT as shown in Figure 2 revealed that its transition temperature was predominantly influenced by macromolecular crowding. This suggests that variations in transition temperatures among the compartments are more likely to be attributed to a difference in macromolecular crowding conditions rather than to actual temperature changes. For an exploratory study, we supposed that the difference of macromolecular crowding in the cytoplasm, mitochondria, and ER was responsible for the difference of transition temperatures in them, and we worked out the most likely macromolecular crowding conditions in the compartments in terms of equivalent Ficoll PM70 concentration. Specifically, we compared the temperature/Ficoll PM70 response curves taken by in vitro spectroscopy measurement (Figure 2e) and the temperature response curves in the intracellular compartments (Figures 3c and 4c,d) and performed maximum likelihood calculations (Note S1, Figure S2). This analysis showed that the macromolecular crowding conditions in the cytoplasm, mitochondria, and ER were equivalent to 16.7, 10.6, and 21.6% Ficoll PM70, respectively. This result suggests that the effect of macromolecular crowding in each intracellular compartment may often need to be carefully checked or compensated for in temperature measurements when using a GETI.

In tsGFP, the coiled-coil formation in the TlpA region at low temperatures favorably stabilizes the phenol form of the GFP chromophore (absorption peak wavelength, 400 nm). Conversely, the unfolding of the coiled coil at high temperatures stabilizes the phenolate form (absorption peak wavelength, 480 nm). The temperature-dependent shift of the equilibrium between these results in a temperature-dependent change in the excitation spectrum.[6] For gMELT, the temperature sensitivity was significantly enhanced because the FRET efficiency between CFP and YFP changed with TlpA dimerization and dissociation in an all-or-none manner. Furthermore, tsGFP, as an excitation ratiometric indicator, requires the temporally sequential acquisition of fluorescence images at two excitation wavelengths. In contrast, gMELT, as an emission ratiometric indicator, enables simultaneous acquisition at two emission wavelengths using a device such as a dual view optic.[28] In this perspective, ratiometric measurements are less susceptible to the diffusion and transport of gMELT than those of tsGFP. As an additional advantage, gMELT, a fluorescence emission ratiometric indicator, is less susceptible to fluctuations in excitation light power, unlike excitation ratiometric measurement observed in tsGFP. Piraner et al. developed a pair of mutated TlpA polypeptide; one chain was anchored to the inner side of the mammalian plasma membrane, and the other chain was fused to a red fluorescent protein (RFP). They observed temperature-dependent localization of the RFP on the membrane.[22] Ratiometric measurement with gMELT is likely to facilitate a more quantitative analysis of temperature-dependent phenomena.

Visualization of Thermogenesis in Mitochondria and ER. To examine the applicability of gMELT for monitoring endogenous thermogenesis, we tried to visualize thermogenesis in mitochondria and ER, which has been previously reported[5,12,39,30].

https://doi.org/10.1021/acssensors.3c02658
ACS Sens. 2024, 9, 3889−3897

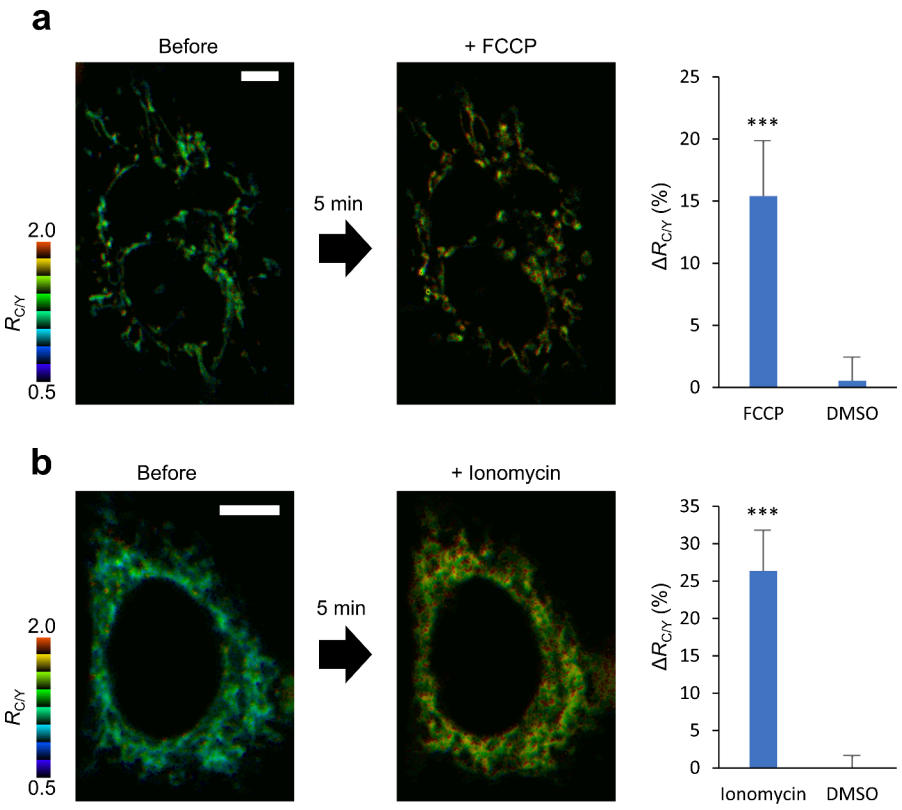

Figure 5. Visualization of heat production in mitochondria or ER of HeLa cells by chemical stimulations. (a) Fluorescent responses to 10 μM FCCP in HeLa cells expressing gMELT-Mito at 35 °C. Left: pseudocolor images of fluorescence ratio $R_{C/Y}$ before and after FCCP treatment. Right: ratio changes ($\Delta R_{C/Y}$) after FCCP application (n = 42 or 41 cells for 0.1% DMSO vehicle or FCCP, respectively; *** $p = 4.8 \times 10^{-22}$ by Student's t test). (b) Fluorescent responses to 5 μM ionomycin in HeLa cells expressing gMELT-ER at 36 °C. Left: pseudocolor images of $R_{C/Y}$ before and after ionomycin treatment. Right: $\Delta R_{C/Y}$ after ionomycin application (n = 44 or 54 cells for 0.1% DMSO vehicle or ionomycin, respectively; *** $p = 5.8 \times 10^{-30}$ by Student's t test). Scale bars indicate 10 μm.

We stimulated HeLa cells expressing gMELT-Mito with carbonyl cyanide 4-(trifluoromethoxy)phenylhydrazone (FCCP), which uncouples oxidative phosphorylation in mitochondria. $R_{C/Y}$ was observed to increase 5 min after the addition of 5 μM FCCP, and the $R_{C/Y}$ increase ($\Delta R_{C/Y}$) was 15.4 ± 4.4% at a medium temperature of 35 °C (Figure 5a). Two-tailed Student's t test led to $p = 4.8 \times 10^{-22}$, comparing between $\Delta R_{C/Y}$ in FCCP- and DMSO-treated cells, indicating the significance of $\Delta R_{C/Y}$ in FCCP-treated cells. Assuming that the $\Delta R_{C/Y}$ ratio change was due to temperature variation, the estimated average temperature change was 0.70 ± 0.12 °C (mean ± SD). The SD was derived using error propagation:

$$\sigma(T)^2 = (\partial R_{C/Y}/\partial T)^{-2}(\sigma_{cell}(R_{C/Y})^2 + \sigma_{cal}(R_{C/Y}(T))^2)$$

where $\sigma(T)$ represents the SD of estimated temperature, $\sigma_{cell}(R_{C/Y})^2$ is the SD of $R_{C/Y}$ over cells, and $\sigma_{cal}(R_{C/Y}(T))^2$ is the SD from calibration errors in Figure 4d. Both $(\partial R_{C/Y}/\partial T)$ and $\sigma_{cal}(R_{C/Y}(T))$ values were estimated through linear interpolation of the data points.

We also tried to observe thermogenesis in HeLa cells expressing gMELT-ER via Ca^{2+} influx induced by the addition of ionomycin, a Ca^{2+} uncoupler. A significant increase of $R_{C/Y}$ was observed 5 min after ionomycin stimulation at a medium temperature of 36 °C ($\Delta R_{C/Y}$ = 26.3 ± 5.4%, $p = 5.8 \times 10^{-30}$ by Student's t test). Attributing this $\Delta R_{C/Y}$ ratio change to a temperature variation, the average temperature increase calculated was 0.78 ± 0.15 °C (mean ± SD), with the SD derived as described above by using error propagation.

The estimated temperature increases in mitochondria and ER were comparable to those previously reported (≃1 °C).[5,12,29,30] However, it is important to recognize that environmental factors such as macromolecular crowding can affect the readouts as a limitation of gMELT. Assuming that the ΔRs in Figure 5b,e were solely due to changes in the crowding, we calculated the ΔR values for mitochondria and ER, and the ΔR values corresponded to an equivalent Ficoll PM70 concentration change of 2.5% (w/w) for both. This estimation used the formula $\Delta c = \Delta R \cdot (dR/dc)^{-1}$, where Δc represents the change in Ficoll PM70 concentration and (dR/dc) was estimated from Figure 2e through linear interpolation of the data points. Although the response of intracellular macromolecular crowding to external stimuli in mitochondria and ER is not well understood, our previous observations indicated no significant changes in macromolecular crowding in the cytoplasm following ionomycin stimulation.[13] To enhance our understanding of intracellular thermogenesis, we expect the development of methods capable of observing the intracellular crowding environment at the organelle level in the future. Studying thermogenesis using gMELT along with assessing factors, such as macromolecular crowding, should advance the boundaries of intracellular thermogenesis studies.

https://doi.org/10.1021/acssensors.3c02658
ACS Sens. 2024, 9, 3889−3897

CONCLUSIONS

We developed a FRET-based highly thermosensitive GETI, gMELT, that can be localized in targeted cellular compartments in mammalian cells. For the improvement of the temperature sensitivity, gMELT took advantage of the heterodimerization behavior of the mutated TlpA pair fused to the FPs of the FRET pair. The fluorescence ratio of the FPs reflected the surrounding temperature. gMELT showed 2-fold higher temperature sensitivity in the cytoplasm, 12-fold higher in the endoplasmic reticulum, and 10-fold higher in the mitochondria than previous sensitive GETIs, indicating the potential to clearly capture the thermogenesis at the organelle level. To examine the capability of capturing endogenous thermogenesis, we observed changes in the fluorescence ratio in mitochondria and ER upon external stimulations previously reported to cause temperature increases in these organelles.[5,12,29,30] The estimated degrees of temperature increases were comparable to those in these reports, assuming that the observed signal changes were exclusively due to temperature variations. Here, it is important to note that gMELT exhibits a dependence on macromolecular crowding in vitro. To deepen our understanding of thermogenic phenomena using gMELT, it is necessary to consider environmental factors, including macromolecular crowding, in addition to the temperature.

Heterogeneous temperature distribution in cells and organelles remains controversial. Although experimental studies on cellular temperatures using nanothermometers have suggested intracellular temperature increase of >1 °C by thermogenesis in cells, they have been sometimes questioned in theoretical aspects. Baffou et al. pointed out that factors other than temperature may be responsible for signal changes in nanothermometers and thus the inaccurate estimation of temperature,[31] and the discussion is still controversial. Because of its higher temperature sensitivity than previously known GETIs and capability for specific organelle localization, gMELT should be useful for the verification and further investigation of thermogenic phenomena.

ASSOCIATED CONTENT

Supporting Information

The Supporting Information is available free of charge at https://pubs.acs.org/doi/10.1021/acssensors.3c02658.

Temperature imaging of quick temperature rise in live HeLa cells with a local heat spot; comparative study of temperature response of gMELT in cells and that of purified gMELT in the presence of macromolecular crowding regent; methods for analysis of macromolecular crowding in intracellular compartments; and nucleotide sequence of gMELT variants (PDF)

Timelapse observation of quick temperature rise in live HeLa cells with a local heat spot (MP4)

AUTHOR INFORMATION

Corresponding Author

Takeharu Nagai − *SANKEN, The University of Osaka, Ibaraki, Osaka 567-0047, Japan; OTRI, The University of Osaka, Suita, Osaka 565-0871, Japan; Research Institute for Electronic Science, Hokkaido University, Sapporo, Hokkaido 001-0021, Japan;* orcid.org/0000-0003-2650-9895; Phone: +81-6-6879-8480; Email: ng1@sanken.osaka-u.ac.jp

Authors

Shun-ichi Fukushima − *SANKEN, The University of Osaka, Ibaraki, Osaka 567-0047, Japan*

Tetsuichi Wazawa − *SANKEN, The University of Osaka, Ibaraki, Osaka 567-0047, Japan;* orcid.org/0000-0002-4171-585X

Kazunori Sugiura − *SANKEN, The University of Osaka, Ibaraki, Osaka 567-0047, Japan*

Complete contact information is available at: https://pubs.acs.org/10.1021/acssensors.3c02658

Author Contributions

S.F. and T.N. conceived the idea and designed the experiments. S.F. performed the experiments. K.S. and T.W. helped with the experiments. S.F. drafted the manuscript, and all authors have given approval to the final version of the manuscript.

Notes

The authors declare no competing financial interest.

ACKNOWLEDGMENTS

The authors acknowledge the support from CREST (JPMJCR15N3 to T.N.), JST, Japan; a Grant-in-Aid for Scientific Research on Innovative Areas (18H05410 to T.N.), JSPS, Japan; a Grant-in-Aid for Scientific Research (C) (22K04891 to T.W.), JSPS, Japan; and a Grant-in-aid for Early-Career Scientists (19K16179 to S.F.).

ABBREVIATIONS

FNT;fluorescence nanothermometry; FP;fluorescent protein; GETI;genetically encoded temperature indicator; ELP;elastin-like polypeptide; gMELT;genetical system to monitor the events of local temperature; FRET;Förster resonance energy transfer; ER;endoplasmic reticulum; FCCP;cyanide 4-(trifluoromethoxy)phenylhydrazone

REFERENCES

(1) Feng, G.; Zhang, H.; Zhu, X.; Zhang, J.; Fang, J. Fluorescence thermometers: intermediation of fundamental temperature and light. *Biomater. Sci.* **2022**, *10*, 1855−1882.

(2) Okabe, K.; Sakaguchi, R.; Shi, B.; Kiyonaka, S. Intracellular thermometry with fluorescent sensors for thermal biology. *Pflugers Arch. Eur. J. Physiol.* **2018**, *470*, 717−731.

(3) Wang, F.; Han, Y.; Gu, N. Cell temperature measurement for biometabolism monitoring. *ACS Sensors* **2021**, *6*, 290−302.

(4) Bai, T.; Gu, N. Micro/nanoscale thermometry for cellular thermal sensing. *Small* **2016**, *12*, 4590−4610.

(5) Okabe, K.; Inada, N.; Gota, C.; Harada, Y.; Funatsu, T.; Uchiyama, S. Intracellular temperature mapping with a fluorescent polymeric thermometer and fluorescence lifetime imaging microscopy. *Nat. Commun.* **2012**, *3*, 705.

(6) Kiyonaka, S.; et al. Genetically encoded fluorescent thermosensors visualize subcellular thermoregulation in living cells. *Nat. Methods* **2013**, *10*, 1232−1238. Kiyonaka, S.; Kajimoto, T.; Sakaguchi, R.; Shinmi, D.; Omatsu-Kanbe, M.; Matsuura, H.; Imamura, H.; Yoshizaki, T.; Hamachi, I.; Morii, T.; Mori, Y. Genetically encoded fluorescent thermosensors visualize subcellular thermoregulation in living cells. *Nat. Methods* **2013**, *10*, 1232−1238.

(7) Chrétien, D.; Bénit, P.; Ha, H.-H.; Keipert, S.; El-Khoury, R.; Chang, Y.-T.; Jastroch, M.; Jacobs, H. T.; Pustin, P.; Rak, M. Mitochondria are physiologically maintained at close to 50 °C. *PLoS Biol.* **2018**, *16* (1), No. e2003992.

(8) Kriszt, R.; Arai, S.; Itoh, H.; Lee, M. H.; Goralczyk, A. G.; Ang, X. M.; Cypess, A. M.; White, A. P.; Shamsi, F.; Xue, R.; et al. Optical

visualisation of thermogenesis in stimulated single-cell brown adipocytes. *Sci. Rep.* **2017**, *7*, 1383.
(9) Nakano, M.; Arai, Y.; Kotera, I.; Okabe, K.; Kamei, Y.; Nagai, T. Genetically encoded ratiometric fluorescent thermometer with wide range and rapid response. *PLoS One* **2017**, *12* (2), No. e0172344.
(10) Savchuk, O. A.; Silvestre, O. F.; Adão, R. M. R.; Nieder, J. B. GFP fluorescence peak fraction analysis based nanothermometer for the assessment of exothermal mitochondria activity in live cells. *Sci. Rep.* **2019**, *9*, 7535.
(11) Homma, M.; Takei, Y.; Murata, A.; Inoue, T.; Takeoka, S. A ratiometric fluorescent molecular probe for visualization of mitochondrial temperature in living cells. *Chem. Commun.* **2015**, *51*, 6194−6197.
(12) Arai, S.; Lee, S. C.; Zhai, D.; Suzuki, M.; Chang, Y. T. A molecular fluorescent probe for targeted visualization of temperature at the endoplasmic reticulum. *Sci. Rep.* **2014**, *4*, 6701.
(13) Vu, C. Q.; Fukushima, S.-i.; Wazawa, T.; Nagai, T. A highly-sensitive genetically encoded temperature indicator exploiting a temperature-responsive elastin-like polypeptide. *Sci. Rep.* **2021**, *11*, 16519.
(14) Pastuszka, M. K.; Janib, S. M.; Weitzhandler, I.; Okamoto, C. T.; Hamm-Alvarez, S.; macKay, A. A tunable and reversible platform for the intracellular formation of genetically engineered protein microdomains. *Biomacromolecules* **2012**, *13*, 3439−3444.
(15) Goedhart, J.; von Stetten, D.; Noiclerc-Savoye, M.; Lelimousin, M.; Joosen, L.; Hink, M. A.; van Weeren, L.; Gadella, W. J., Jr.; Royant, A. Structure-guided evolution of cyan fluorescent proteins towards a quantum yield of 93%. *Nat. Commun.* **2012**, *3*, 751.
(16) Yoshioka-Kobayashi, K.; Matsumiya, M.; Niino, Y.; Isomura, A.; Kori, H.; Miyawaki, A.; Kageyama, R. Coupling delay controls synchronized oscillation in the segmentation clock. *Nature* **2020**, *580*, 119−123.
(17) Nagai, T.; Yamada, S.; Tominaga, T.; Ichikawa, M.; Miyawaki, A. Expanded dynamic range of fluorescent indicators for Ca2+ by circularly permuted yellow fluorescent proteins. *Proc. Natl. Acad. Sci. U. S. A.* **2004**, *101*, 10554−10559.
(18) Fu, C.; Donovan, W. P.; Shikapwashya-Hasser, O.; Ye, X.; Cole, R. H. Hot fusion: An efficient method to clone multiple DNA fragments as well as inverted repeats without ligase. *PLoS One* **2014**, *9* (12), No. e115318.
(19) Fang, J.; Yi, S.; Simmons, A.; Tu, G. H.; Nguyen, M.; Harding, T. C.; VanRoey, M.; Jooss, K. An antibody delivery system for regulated expression of therapeutic levels of monoclonal antibodies in vivo. *Mol. Ther.* **2007**, *15*, 1153−1159.
(20) Hurme, R.; Berndt, K. D.; Normark, S. J.; Rhen, M. A proteinaceous gene regulatory thermometer in Salmonella. *Cell* **1997**, *90*, 55−64.
(21) Kotera, I.; Iwasaki, T.; Imamura, H.; Noji, H.; Nagai, T. Reversible dimerization of *Aequorea victoria* fluorescent proteins increases the dynamic range of FRET-based indicators. *ACS Chem. Biol.* **2010**, *5*, 215−222.
(22) Piraner, D. I.; Wu, Y.; Shapiro, M. G. Modular thermal control of protein dimerization. *ACS Synth. Biol.* **2019**, *8*, 2256−2262.
(23) Piraner, D. I.; Abedi, M. H.; Moser, B. A.; Lee-Gosselin, A.; Shapiro, M. G. Tunable thermal bioswitches for in vivo control of microbial therapeutics. *Nat. Chem. Biol.* **2017**, *13*, 75−80.
(24) Boersma, A. J.; Zuhorn, I. S.; Poolman, B. A sensor for quantification of macromolecular crowding in living cells. *Nat. Methods* **2015**, *12*, 227−229.
(25) Kim, J. H.; Lee, S.-R.; Li, L.-H.; Park, H.-J.; Park, J.-H.; Lee, K. Y.; Kim, M.-K.; Shin, B. A.; Choi, S.-Y. High cleavage efficiency of a 2A peptide derived from porcine teschovirus-1 in human cell lines, zebrafish and mice. *PLoS One* **2011**, *6*, No. e18556.
(26) Lu, K.; Wazawa, T.; Sakamoto, J.; Vu, C. Q.; Nakano, M.; Kamei, Y.; Nagai, T. Intracellular Heat Transfer and Thermal Property Revealed by Kilohertz Temperature Imaging with a Genetically Encoded Nanothermometer. *Nano Lett.* **2022**, *22*, 5698−5707.
(27) Nwokolo, O. A.; Kidd, B.; Allen, T.; Minasyan, A. S.; Vardelly, S.; Johnson, K. D.; Nesterova, I. V. Rational Design of Memory-Based Sensors: the Case of Molecular Calorimeters. *Angew. Chem., Int. Ed. Engl.* **2021**, *60*, 1610−1614.
(28) Kinosita, K.; Itoh, H.; Ishiwata, S.; Hirano, K.; Nishizaka, T.; Hayakawa, T. Dual-view microscopy with a single camera: real-time imaging of molecular orientations and calcium. *J. Cell Biol.* **1991**, *115*, 67−73.
(29) Gota, C.; Okabe, K.; Funatsu, T.; Harada, Y.; Uchiyama, S. Hydrophilic Fluorescent Nanogel Thermometer for Intracellular Thermometry. *J. Am. Chem. Soc.* **2009**, *131*, 2766−2767.
(30) Suzuki, M.; Tseeb, V.; Oyama, K.; Ishiwata, S. Microscopic detection of thermogenesis in a single HeLa cell. *Biophys. J.* **2007**, *92*, L46−L48.
(31) Baffou, G.; Rigneault, H.; Marguet, D.; Jullien, L. A critique of methods for temperature imaging in single cells. *Nat. Methods* **2014**, *11*, 899−901.

https://doi.org/10.1021/acssensors.3c02658
ACS Sens. 2024, 9, 3889−3897